Related Flavonoids Cause Cooperative Inhibition Of The Sarcoplasmic Reticulum Ca^{2+} ATPase By Multimode Mechanisms.

Oluseye A. Ogunbayo[1,2] & Francesco Michelangeli [1]

[1]School of Biosciences, University of Birmingham, Edgbaston, Birmingham. B15 2TT, UK;

[2]Centre for Integrative Physiology, School of Biomedical Sciences, University of Edinburgh, UK.

Running title: *Inhibition of the Ca^{2+} ATPase by flavonoids*

To whom correspondence should be addressed: Dr F. Michelangeli, School of Biosciences, University of Birmingham, Edgbaston, Birmingham, UK, B15 2TT; Email: F.Michelangeli@bham.ac.uk; Tel: +44-121-4145983

Keywords: Ca^{2+}ATPase, flavonoids, quercetin, SERCA, cooperative inhibition.

ABSTRACT

Flavonoids are group of plant-derived hydroxylated polycyclic molecules found in fruit and vegetables. They are known to bio-accumulate within humans and are believed to have beneficial health effects including cancer chemo-protection. One mechanism that has been proposed to explain this is that they are able to induce apoptosis in cancer cells by inhibiting a variety of kinases and also the Ca^{2+}ATPase. An investigation into the mechanism of inhibition of 3 flavonoids, quercetin, galangin and 3,6 dihydroxyflavone (3,6-DHF) was undertaken. Each inhibited the Ca^{2+}ATPase with Ki values of 8.7 μM, 10.3 μM and 5.4 μM, respectively, showing cooperative inhibition with n~2. Given their similar structures, the flavonoids showed several differences in their mechanisms of inhibition. All three flavonoids stabilized the ATPase in the E1 conformation and reduced [^{32}P]-ATP binding. However, both galangin and 3,6-DHF increased Ca^{2+} affinity to the ATPase by decreasing the Ca^{2+}-dissociation rate constant, while quercetin had little effect. Ca^{2+}-induced changes in tryptophan fluorescence levels were reduced in the presence of 3,6-DHF and galangin (but not with quercetin), indicating that Ca^{2+}-associated changes within the transmembrane helices are altered. Both galangin and quercetin reduced the rates of ATP-dependent phosphorylation and dephosphorylation, while 3,6-DHF did not. Modelling studies suggest that flavonoids could potentially bind to two sites, one directly where nucleotides bind within ATP binding site and the other at a site close by. We hypothesise that interactions of these two neighbouring sites may account for both the cooperative inhibition and the multimode mechanisms of action seen with related flavonoids.

INTRODUCTION

Flavonoids are the most common and widely distributed group of the phytoestrogens, which are found in fruits & vegetables and through their consumption these compounds have been shown to reach concentrations of several micromolar in human blood plasma [1]. These plant-derived compounds are believed to have a range of beneficial properties including cancer chemo-protective properties [2-4]. One reason for this is that flavonoids are able to initiate apoptosis, especially in cancer cells [5, 6]. From recent research the action of flavonoids on cancer cells is likely to be multifaceted and complex, affecting a variety of key molecular targets that inhibit cell proliferation and / or potentiate apoptosis [5,6]. A number of specific targets which are inhibited by flavonoids have been identified as kinases such as cyclin–dependent kinase 6, PI3K/Akt kinase, casein kinase 2 and aurora B kinase [7-10].

Flavonoids have also been shown to inhibit sarcoplasmic / endoplasmic reticulum Ca^{2+}-ATPases (SERCA) [11, 12] and also induce apoptosis via the Ca^{2+}-dependent mitochondrial pathway that can be activated through an exaggerated elevation of cytosolic [Ca^{2+}] [13,14]. Consequently, one hypothesis is that the inhibition of the Ca^{2+}-ATPases causes 'Ca^{2+} overload' of the mitochondria, leading to the opening of the permeability transient pore (PTP) and release of mitochondrial pro-apoptotic factors such as cytochrome c, which ultimately leads to apoptotic cell death [12-14].

Ca^{2+}ATPase bind ATP and undertake phosphorylation, which are also common characteristics found with kinases, and therefore an understanding of the mechanism by which flavonoids inhibit the Ca^{2+} ATPase, may help to indicate generic modes of action with other target enzymes.

In a previous study we investigated a wide range of flavonoids and showed that the number and position of hydroxyl groups within the molecule greatly affect its ability to inhibited Ca^{2+} ATPase activity [12]. From the flavonoids studied the IC_{50} values ranged from low μM for quercetin and galangin to little or no inhibition for primuletin and apigenin [12]. Why such closely related molecules differed so dramatically in their potency was unclear and therefore in this study three potent flavone inhibitors were investigated in order to further elucidate their mechanisms of action.

RESULTS

Figure 1 shows the inhibition of three potent flavonoids on the activity of the rabbit skeletal muscle SR Ca^{2+} ATPase. The inhibition showed relatively poor fits when assuming that the inhibition was due to either single site inhibitor binding or 2 site independent binding. However, excellent fits to the experimental data were achieved when cooperative inhibition was assumed where Hill coefficients were close to 2 for all three flavonoids. Table 1 shows the kinetic parameters for the different inhibition modes. Figure 2 shows the effect of these flavonoids on the dependency of free Ca^{2+} concentration activity of the Ca^{2+} ATPase. In the absence of flavonoids, a typical bell-shaped activity profile is observed which is due, in part, to Ca^{2+} affecting the E1 and E2 states of the Ca^{2+} ATPase [15, 16].

As can be seen in figure 2 good fits to all the experimental data could be achieved using this equation as they had χ^2 values of 0.98 or better. For the Ca^{2+} ATPase in the absence of flavonoids the data best fitted the data assuming a K_s of 0.29 ± 0.05 μM, a K_i of 0.24 ± 0.04 mM and a Vmax of 4.8 ± 0.2 IU/mg (figure 2A). In the presence of 3,6-DHF (6 μM) the Vmax was reduced to 3.1 ± 0.2 μM but the K_s and K_i were

changed little from control (0.29 ± 0.05 μM and 0.21 ± 0.04 mM, respectively) (figure 2A). Quercetin (9 μM) also showed negligible changes in the activity parameters (apart from Vmax) with a K_s of 0.21 ± 0.05 μM and K_i of 0.14 ± 0.04 mM (figure 2B), as did galangin (9 μM) which gave a good fit assuming a K_s of 0.36 ± 0.06 μM and a K_i of 0.16 ± 0.03 mM (figure 2C).

Since the activity of the Ca^{2+} ATPase as a function of free [Ca^{2+}] is not simply related to Ca^{2+} affinity, Ca^{2+} binding can more readily be monitored by observing Ca^{2+}- dependent changes in tryptophan fluorescence of the ATPase [15, 17, 18]. Figure 3 shows the effects of 3,6-DHF (15 μM), quercetin (20 μM) and galangin (20 μM) on the fluorescence changes induced by a range of Ca^{2+} concentrations (10 nM - 0.1 mM) and table 2 shows the apparent K_d for Ca^{2+} binding calculated from figure 3. Also of note is the observation that the degree of tryptophan fluorescence change in the presence of 3,6-DHF and galangin (but not quercetin) are substantially reduced compared to control. From the K_d values it appears that an increase in affinity for Ca^{2+} binding is evident in the presence of 3,6,-DHF and galangin, as the Kd values were statistically lower than for the control with p values of less than 0.1. However although there appeared to be an increase in the Kd value for quercetin compared to control this was not considered significant as the p value was greater than 0.1 To further explore this, the rate constant for Ca^{2+} binding was measured in the presence of these flavonoids, using stopped-flow fluorescence measurements as previously described in [15, 17]. The rate constants for Ca^{2+} binding (k_{on}) are given in table 2. Since the K_d is a measure of the ratio of k_{off} / k_{on}, the k_{off} (Ca^{2+} dissociation rate constant) values for this process were calculated and given in table 2. As can be seen, changes in the Ca^{2+} dissociation rate constants (k_{off}) in the presence of 3,6,-DHF and galangin were observed when compared to control.

Figure 4 shows the biphasic profile of activity for the Ca^{2+} ATPase as a function of [ATP] as previously noted in other studies [15, 19]. The kinetic parameters in the absence of flavonoids was best fitted assuming Km and Vmax for the catalytic site of 0.19 ± 0.11 μM and 1.48 ± 0.23 IU/mg, respectively and a Km and Vmax for the regulatory site of 0.04 ± 0.02 mM and 2.6 ± 0.2 IU/mg, respectively ($\chi^2 = 0.98$). A notable effect of the flavonoids appeared to be on the Km value for ATP binding to the catalytic site (likely indicating changes in ATP binding affinity), whereas in the presence of quercetin (9 μM) or galangin (9 μM) the calculated Km_{cat} values both increased substantially to 3.9 ± 2.0 μM and 2.4 ± 0.3μM, respectively. 3,6-DHF (6 μM), however, had little effect on the Km for the catalytic site (0.21 ± 0.09 μM). In addition, all three flavonoids also substantially increased the Km for the regulatory site, compared to control (the Km_{reg} for quercetin was 0.99 ± 0.33 mM, for 3,6-DHF it was 0.27 ± 0.07 mM and for galangin the value was 0.98 ± 0.39 mM).

In order to further investigate whether these flavonoids affected ATP binding to the Ca^{2+} ATPase, [^{32}P]-ATP binding studies were undertaken with 4μM ATP. As the equivalent of 5 μM Ca^{2+} ATPase was used in these experiments and since this is associated with approximately 200 μM lipid, which may also bind these lipophilic flavonoids, 50 μM of the flavonoids were used in these experiments. Figure 5 shows that all three flavonoids were able to reduce [^{32}P]-ATP binding to the ATPase to some degree, with both galangin and quercetin being substantially better than 3,6-DHF.

In order to determine whether these flavonoids could alter the rate of ATP-dependent phosphorylation (ie E1 + ATP → E1~P + ADP), experiments were undertaken with 5 μM ATP at 3°C to reduce the rate of this fast step [18]. For each flavonoid (30μM), two time points were measured (10 sec and 30 sec), and the level of phospho-enzyme formation of the ATPase determined for each. Figure 6A shows that in the absence of flavonoids by 10 sec the steady state levels of phospho-enzyme formation had been reached since the E~P level was similar to that at the 30 sec time point. A similar result was also observed for 3,6-DHF. However, for both galangin and quercetin the phospho-enzyme levels at 10 sec were considerably lower compared to the values observed at 30 sec, indicating that in the presence of galangin and quercetin the rate of ATP-dependent phosphorylation of the Ca^{2+} ATPase had been significantly reduced.

Dephosphorylation of the Ca^{2+} ATPase in the E2 state (ie E2~P → E2 + Pi) has been shown to be one of the rate limiting steps of the enzymatic cycle. Figure 6B shows the effects of the flavonoids on the dephosphorylation rates. In the absence of flavonoids the dephosphorylation rate constant was calculated to be $0.24 \pm 0.02 s^{-1}$, which was little affected in the presence of 30 μM 3,6-DHF ($k_{obs} = 0.26 \pm 0.02 s^{-1}$). However, both galangin (30 μM) and quercetin (30 μM) substantially reduced the dephosphorylation rate compared to control ($k_{obs} = 0.14 \pm 0.01\ s^{-1}$ and $0.10 \pm 0.02\ s^{-1}$, respectively).

ADP-sensitive and ADP-insensitive forms of the Ca^{2+} ATPase can be studied by allowing the ATPase to be phosphorylated by ATP to a steady state level after which excess ADP is added and a portion of phosphorylated ATPase is able to transfer the phosphate group to ADP and reconvert it back to ATP [11, 18]. The ADP–sensitive form is considered to be that form which is able to undertake the reversal of ATP dependent phosphorylation (ie E1~P.ADP → E1.ATP), while the ADP-insensitive form is either due to the fraction of the ATPase in the E2~P state or due to a state blocked in a E1~P. ADP conformation and unable to reverse back to E1.ATP. Figure 7 shows that under the experimental conditions used and in the absence of flavonoids, the majority of the phosphorylated enzyme can be dephosphorylated back to E1.ATP (ie 94% ADP-sensitive and 6% ADP-insensitive). Little effect, compared to control, is noted with 3,6-DHF (30 μM) and galangin (30 μM). However, in the presence of 30 μM quercetin, the majority

of the phosphorylated ATPase is ADP-insensitive and is little changed upon ADP addition (ie 12% ADP-sensitive and 88% ADP-insensitive).

The E1 → E2 step has been identified as a step which is influenced by many inhibitors such as thapsigargin and BHQ and which stabilize the ATPase in an E2 conformation [20, 21]. One method commonly used to measure this step is where the Ca^{2+} ATPase is covalently labelled with FITC at position Lys 515 within the nucleotide binding domain of the ATPase [21, 22]. By monitoring the fluorescein fluorescence changes when the Ca^{2+}-ATPase is shifted into the E1 conformation by Ca^{2+} or the E2 conformation by vanadate [16, 22], in the presence of the flavonoids, the position of the E1 and E2 equilibrium can be determined [16, 22]. The changes in fluorescence induced by Ca^{2+} and vanadate at pH 6.0 were monitored as under these conditions where the ATPase would predominantly be in an E2 state (ie E1/E2 ratio has been calculated to be 0.14) [22]. Table 3 shows that in the absence of flavonoids the largest change in fluorescence induced by Ca^{2+} is in the absence of the flavonoids as in their presence the fluorescence changes is substantially reduced for all three. However, upon addition of vanadate the opposite effect is observed, with the largest change in fluorescence occurring in the presence of the flavonoids. Taken together these data indicate that all the flavonoids (at 20 μM) cause the Ca^{2+}ATPase to be shifted substantially towards the E1 conformational state, with the E1/E2 ratio increasing substantially compared to control (table 3).

DISCUSSION

Flavonoids occur naturally in a variety of foods, for instance quercetin is found in relatively high levels in watercress, red onions and kale, while galangin is abundant in galangal root. Much research has been focussed on flavonoids recently due to their potent chemo preventative properties in cancer [2-4]. Although the mechanisms by which flavonoids cause these affects both *in-vivo* and *in-vitro* is likely to be multifaceted [23], an understanding of how they interact with and influence the activity of proteins such as the Ca^{2+} ATPase which undertakes a number of molecular processes typically found in many enzymes that regulate key cellular processes such as; Ca^{2+} binding, ATP binding, phosphorylation, dephosphorylation and membrane transduction, may shed some light upon their more generic mechanisms of action with other enzyme targets.

In a previous study we investigated the effects of 25 flavonoids for their inhibitory effects on the Ca^{2+} ATPase activity and noted that only minor changes in the degree hydroxylation or the position of the hydroxyl groups on the flavone ring was required to either make them potent inhibitors of the Ca^{2+}

ATPase (with IC_{50} values in the low μM range) or completely ineffective [12]. In this study we focussed on the mechanisms by which three potent flavonoids, quercetin, galangin and 3,6-DHF cause their inhibition.

Multimode Mechanisms of inhibition

Our main observation in this study is that given the great similarity in both the structure and Ki values of these three flavonoids, their mechanisms of inhibition appeared to be quite different. All three flavonoids exhibited sigmoidal shaped inhibition curves for Ca^{2+} ATPase activity which were best fitted assuming that inhibition was cooperative in nature with Hill coefficients of ~2. This would therefore suggest that there are a number of flavonoid binding sites within the ATPase that contribute to the observed inhibition and that binding of the flavonoid to one of these sites increases the binding of the flavonoid to the other site(s). Although two site inhibitor binding, where two structurally different inhibitors bind to the Ca^{2+}ATPase in a cooperative fashion has previously been reported [24], here we indicated that two (or more) sites exist that are able to bind the same inhibitor and interact with each other cooperatively. This type of cooperative inhibition, where 2 or more sites are able to interact together has only been reported for a few other enzymes [25, 26] and may well also explain why flavonoids affect different steps in the Ca^{2+} ATPase mechanism.

All three flavonoids tested, affected the E1 to E2 conformational step to some degree by preferentially stabilizing the Ca^{2+} ATPase in the E1 state (table 3). All three flavonoids also appeared to affect ATP binding to a greater or lesser degree as well (figure 5). However, in relation to Ca^{2+} binding to the ATPase differences were observed, with 3,6-DHF increasing the affinity for Ca^{2+} binding to the ATPase by about 2-fold through reducing the Ca^{2+} dissociation 'off' rate (figure 3 & table 2). Quercetin, on the other hand, appeared to decrease the Ca^{2+} affinity but this was not statistically significant ($p > 0.1$). The observation that in the presence of 3,6-DHF and galangin the Ca^{2+} -induced tryptophan fluorescence changes were substantially reduced (figure 3) might also indicate that any associated changes within the transmembrane region of the ATPase (where 12 out of 13 tryptophans are located) are reduced, compared to control. A similar result was also observed when mastopan (a peptide venom) inhibited the Ca^{2+} ATPase [17], this showed a reduction in the eversion step (E1~P → E2~P), where appropriate re-arrangements of the transmembrane helices are required.

The effects of flavonoids upon phosphorylation / dephosphorylation (figure 6 A & B) again showed differences, with both galangin and quercetin reducing the rates of both ATP-dependent phosphorylation and dephosphorylation, while 3,6-DHF had no effect upon these steps. In addition, when investigating the reverse reaction where the phosphorylated Ca^{2+} ATPase can donate the phosphate back to ADP, in order

to determine the steady levels of ADP-sensitive or ADP-insensitive forms, only quercetin showed any difference compared to control, by effectively reducing the amount of the Ca^{2+} ATPase in the ADP-sensitive form (figure 7). It is unlikely from our other results that the ATPase in the presence of quercetin is preferentially stabilized in a E2~P state which might be expected from this result. Rather given the fact that quercetin reduces ATP binding and phosphorylation rates the most likely explanation is that quercetin stabilizes The E1~P form stopping it from reversing back to the unphosphorylated E1form.

Molecular modelling predicts two hypothetical flavonoid binding sites that could account for multimode cooperative inhibition.

All three flavonoids contain a hydroxyl group at the 3 position on ring C which has been shown to twist ring B with respect to rings A and C giving these flavonoids a 'kinked' rather than planer conformation [27]. Figure 8A shows very close structural overlap between the 'kinked' flavonoid and ADP (in the conformation adopted when bound to the ATPase), with the B ring on the flavonoid superimposing well with the adenine ring and the C ring (pyran ring) of flavonoid superimposing closely with the furan ring (ribose) of ADP. Molegro Virtual Docker 2007 was then used to locate potential flavonoid (quercetin) binding sites on the Ca^{2+} ATPase using the E1.ADP bound conformational structure (PBD code 1WPE). The most frequently predicted area for binding was within the nucleotide binding domain. Aided by manual fine tuning, these predicted sites highlighted two potential non-overlapping locations, directly within, and very close to, the nucleotide binding (N) site (designated sites 1 and 2 in figure 8B). At site 1 the flavonoid occupies the same space and position as ADP does within the crystal structure. Detailed analysis of site 1 shows that the flavonoid has the potential to form hydrogen bonds (H-bonds) with a number of key amino acid residues (figure 8C). For instance Thr441 and Arg560 may form potential H-bonds with the C ring of quercetin, while Gly626 may form H-bonds with a hydroxyl group on the A ring and Glu442 and Lys515 for H-bonds with the B ring. Interestingly several of these residues, from mutagenesis and crystallographic studies, are also known to interact with ATP or ADP [28, 29]. Figure 8D shows the location of ADP with the crystal structure. In addition, aromatic ring stacking between the B ring and Phe487 is also predicted in this model, which is again similar to that observed for the adenine ring of ADP and Phe487 within the crystal structure (figure 8D) [28]. Arg560 interacts with the β-phosphate group of ATP and is essential for both ATP binding, and maintaining an E1 conformation [28, 29]. In addition, mutating either Arg560 or Gly626 residues decreases ATP-dependent phosphorylation levels [28, 29] while Gly626 also greatly affects Pi-dependent phosphorylation of the E2 state. Also mutating Phe487 inhibits ATP binding [30]. If the interactions of these specific amino acid residues are altered by flavonoids binding within this region of the ATPase, it would be feasible that this would have profound affects upon ATP- binding, phosphorylation and E1 stabilization.

Figure 8E shows the predicted location of the flavonoid at site 2 which is located at the interface between the nucleotide binding domain and the actuator domain (see figure 8A). Also shown in figure 8E is the location of ADP. Although both sites do not overlap (and thus both could be occupied) there are clearly some amino acid residues that are shared by both sites, and this could well contribute to cooperative binding / inhibition. Furthermore, at this site the B ring of the flavonoid can also interact with several amino acid residues located within the actuator domain (A-domain). As this domain is required to undergo a substantial rotation and movement in order to cause the E1 conformation to go into the E2 conformation, it could be envisaged that the flavonoid binding at site 2 may block this motion and therefore stabilise the E1 form. The existence of a second non nucleotide binding site can also be inferred from the fact that previous studies have also shown that when Lys 515 is covalently modified with FITC, ATP and other nucleotides are unable to bind [31]. However, since all three flavonoids are able to affect Ca^{2+} induced changes in FITC fluorescence associated with the E2 to E1 transition (table 3), this must indicate that they can bind to sites other than nucleotide binding site (ie site 1), and site 2 is located well away from Lys515.

In order to explain both cooperative inhibition and the multimode mechanisms of inhibition between these structurally related flavonoids it could be hypothesised that flavonoids can bind in a cooperative fashion to 2 (or more) neighbouring sites on the Ca^{2+} ATPase and depending upon the order of binding to these sites and the degree of occupation, dictated by the flavonoid structure, it can be envisaged that different steps will be affected during the enzymatic cycle. However, proof of this hypothesis will only be confirmed through future crystallographic studies.

In summary, some flavonoids have the ability to alter ATP binding properties, phosphorylation and dephosphorylation of the Ca^{2+} ATPase by binding to several sites possibly close to the ATP binding site. The occupation of these sites is likely to be cooperative in nature and their order of occupancy or degree of occupancy may well be dependent upon their structure, leading to altered mechanisms of inhibition.

Furthermore, the modulation of the nucleotide binding domain by flavonoids which are known to affect kinase activity that control a wide range of important cellular processes, may also occur. Indeed a precedent for this has recently been confirmed through enzymological, crystallographic and modelling studies of a plant derived casein kinase 2 which was shown to bind the flavonoid luteolin within its ATP binding domain [9].

MATERIALS AND METHODS

Flavonoids (purity ≥ 97 %) were purchased from Sigma/ Aldrich (St Louis, MO, USA). All other reagents were of analytical grade. Flavonoids were also dissolved in dimethyl sulfoxide (DMSO, Sigma) and the solution was never more than 1 % (v/v) in the assays performed. Native sarcoplasmic reticulum (SR) Ca^{2+} ATPase (**EC 3.6.3.8**) was prepared from rabbit skeletal muscle as described in Michelangeli and Munkonge (1991) [32] and typically had a purity of approximately 80-90 %.

SERCA activity

The effects of flavonoids on SERCA activity were investigated as a function of Ca^{2+} and ATP concentration, employing a coupled enzyme assay method at pH 7.2 as previously described in [16, 32]. Typically, between 11-22 μg/ ml of SERCA was added to a buffer containing 40 mM Hepes/KOH (pH 7.2), 5 mM $MgSO_4$, 0.42 mM phosphoenolpyruvate, 0.15 mM NADH, 8.0 U pyruvate kinase, 20 U lactate dehydrogenase, 1.01 mM EGTA and 2.1 mM ATP (unless otherwise stated). In all experiments, unless otherwise stated, a free Ca^{2+} concentration of 6 μM (pCa 5.2) was used. Free Ca^{2+} concentrations were calculated as described in Gould et al. (1986) [33].

Inhibition data were fitted using the following equations:

(i) For single site inhibitor binding:

$$V=Vmax / (1 + [I] / Ki)$$

where V is activity, Vmax is the maximal activity achieved under the experimental conditions and K_i the inhibitory constant.

(ii) For independent 2-site inhibitor binding:

$$V= [Vmax / (1 + [I] / Ki^A) + Vmax / (1 + [I] / Ki^B)]-Vmax$$

where V is activity, Vmax is the maximal activity achieved under the experimental conditions and Ki^A and Ki^B are the inhibitory constants for site A and site B, respectively.

(iii) For cooperative inhibitor binding:

$$V= Vmax / (1 + [I]^n / Ki^n)$$

where V is activity, Vmax is the maximal activity achieved under the experimental conditions and K_i the inhibitory constant and n is the cooperativity coefficient which can relate to the number of binding sites.

The activity profiles as a function of free [Ca^{2+}] can be adequately modelled assuming Ca^{2+} causes stimulation at low [Ca^{2+}] and inhibits at higher Ca^{2+} concentrations, using the following equation:

$$\text{Activity} = (V_{max} \times [Ca^{2+}] / (K_s + [Ca^{2+}])) + (V_{max} / (1 + [Ca^{2+}] / K_i)) - V_{max}$$

where Vmax is the maximal activity achieved under the experimental conditions, K_s is the stimulatory phase constant and K_i the inhibitory phase constant [15,16].

The biphasic activity profiles as a function of [ATP] can be modelled assuming a bi-Michaelis Menten process, where ATP independently interacts with high affinity catalytic and lower affinity regulatory sites [15,19], using the following equation:

$$\text{Activity} = (Vmax_{cat} \times [ATP] / Km_{cat} + [ATP]) + ([Vmax_{reg} \times [ATP] / Km_{reg} + [ATP])$$

where $Vmax_{cat}$, Km_{cat}, $Vmax_{reg,\ and}$ Km_{reg} are kinetic parameters for the catalytic site and regulatory site, respectively.

Intrinsic tryptophan fluorescence measurements to monitor Ca^{2+}-induced conformational changes of Ca^{2+}ATPase

The conformational change induced by the addition of Ca^{2+} to the ATPase was monitored by observing the change in intrinsic tryptophan fluorescence as described in [15, 17]. 50 μg/ ml ATPase (in the absence and presence of flavonoids) was added to a buffer containing 20 mM Hepes/Tris, 100 mM $MgSO_4$, 1 mM EGTA (pH 7.0) and the induced-conformational change was measured as a percentage change in total tryptophan fluorescence, over a range of free [Ca^{2+}] (10nM – 100 μM), at 25 °C (excitation 285 nm, emission 325 nm).

Measurement of the transient kinetics of the conformational changes associated with Ca^{2+}-binding

Rapid kinetic fluorescence measurements were performed using a stopped-flow fluorescence spectrophotometer (Applied Photophysics, UK, model SX-17MV) as described in [15, 17]. The sample handling unit possesses two syringes, A and B (drive ratio 10:1), which are driven by a pneumatic ram. In the Ca^{2+} binding experiments, syringe A, containing the Ca^{2+}-ATPase (1 μM) in 20 mM Hepes/Tris (pH 7.2), 100 mM KCl, 5 mM $MgSO_4$, 50 μM EGTA was rapidly mixed with syringe B, containing 1 mM

Ca^{2+} (final concentration). Tryptophan fluorescence was monitored at 25 °C by exciting the sample at 280 nm and measuring the emission above 320 nm using a cut off filter.

FITC-labelled ATPase measurements

SR Ca^{2+}-ATPase was labelled with fluorescein 5'-isothiocyanate (FITC), according to the method described in [18, 22] to monitor the E2 → E1 transition. The Ca^{2+}-ATPase (1.1 mg/ml) was added in equal volume to the starting buffer (1 mM KCl, 250 mM sucrose and 50 mM potassium phosphate pH 8.0). FITC in dimethylformamide was then added at a molar ratio of FITC/ATPase of 0.5: 1. The reaction was incubated for 1 hr. at 25 °C and stopped by the addition of 250 µl of 0.2 M sucrose, 50 mM Tris/HCl pH 7.0, which was left to incubate for 30 min at 30 °C prior to being placed on ice until required. Fluorescence measurements of FITC-ATPase were made in a buffer containing 50 mM Tris, 50 mM maleate, 5 mM $MgSO_4$, 100 µM EGTA and 100 mM KCl at pH 6.0. Fluorescence was measured in a PerkinElmer LS50B fluorescence spectrophotometer at 25 °C (excitation 495 nm, emission 525 nm). Ca^{2+} (400 µM) or vanadate (100 µM) was then added to induce changes in fluorescence intensity. The E1/E2 ratio was calculated from Ca^{2+} induced fluorescence changes as described in [22], assuming that the E1/E2 ratio at pH 6.0 under control conditions is 0.14 [22].

[^{32}P]-ATP binding

These experiments were undertaken at 3 °C in a 150mM TES / Tris buffer containing 2 mM $MgSO_4$, pH 7.0 and also containing 3mM EGTA to avoid phosphorylation. The buffer contained 4 µM ATP which was doped with [^{32}P]-ATP (125Ci/mol) and 0.5mg/ml Ca^{2+} ATPase. The buffer also contained the presence or absence of 50 µM flavonoids. 0.5 ml of this mixture were then rapidly filtered through a 0.45 µm filter and then added to 4 ml of Ultima flow scintillant and the radiation determined using liquid scintillation spectrometry. The non-specific values were determined by filtering 0.5ml of the labelled buffer alone and these values were subtracted from the values in the presence of the Ca^{2+} ATPase.

ATP-dependent phosphorylation

The rate of ATP-dependent phosphorylation of the Ca^{2+} ATPase was measured as described in [18], but at pH 7.0 and 3 °C in order to slow down the rate. The experiment was initiated by addition of 5 µM [^{32}P]ATP (specific activity 20 Ci/ mol). After 10 secs or 30 secs the samples were quenched with 250 µl of 40 % trichloroacetic acid / 0.2 M H_3PO_4. The protein was then left to precipitate on ice for 30 mins, after which it was filtered through Whatman GF/C filters, washed and left to dry. Finally, the filters were added to 4 ml of Ultima flow scintillant and the radioactivity of each sample determined using liquid scintillation spectrometry.

Measurement of phosphoenzyme decay by pulse-chase technique

To measure the rate of phosphoenzyme decay, a pulse chase experiment based on the method described in [16] was employed. Briefly, Ca^{2+} -ATPase (0.15 mg/ ml) was suspended in a buffer containing 20 mM Mops/KOH (pH 7.0), 80 mM KCl, 10 mM $MgCl_2$, 1 mM EGTA at a temperature of 3 ºC. Ca^{2+} was added to give a free [Ca^{2+}] of 5 μM based on the constants given in [33]. The experiment was initiated by addition of 5 μM [^{32}P]-ATP (specific activity 20 Ci/ mol). The assay was incubated for 10 secs prior to addition of 0.5 mM non radioactive ATP. 0.5 ml of the assay was then removed and stopped at various times (0- 20 secs) by addition of 250 μl 40% (w/ v) trichloroacetic acid/ 0.2 M H_3PO_4. Following this, 0.25 mg BSA was added to each assay, and the samples were placed on ice for 30 minutes to allow precipitation. The precipitation was collected by rapid filtration through Whatman GF/C filters and washed with 30 ml of 12 % (w/ v) trichloroacetic acid / 0.2 M H_3PO_4. The filters were left to dry and then placed in scintillant and counted

Ratio of ADP-sensitive to ADP-insensitive forms of the Ca^{2+}-ATPase

The ratio of ADP-sensitive to ADP-insensitive forms of the Ca^{2+}-ATPase was measured as described by [18]. The experiment was performed at 3 ºC in 20 mM Hepes/Tris (pH 7.2) containing 100 μM KCl, 50 μM $MgSO_4$, 50 μM $CaCl_2$ and 0.1 mg/ ml ATPase in a total volume of 10 ml. Phosphorylation of the ATPase was initiated by the addition of 20 μM [^{32}P]ATP (20 Ci/mol). Following incubation for up to 40 secs, ADP solution was added (final concentration of 1.5 mM) to determine the proportion of the ADP-sensitive enzyme. 1 ml samples were taken at regular intervals both before and after ADP addition and quenched with 250 μl of 40 % trichloroacetic acid/ 0.2 M H_3PO_4. The protein was then left to precipitate on ice for 30 mins, after which it was filtered, washed and left to dry. Finally, the filters were added to 4 ml of Ultima flow scintillant and the radioactivity of each sample determined using liquid scintillation spectrometry.

Data fitting and statistics

Fig P (Biosoft) was used to fit the experimental data to appropriate equations, determine parameters and constants and calculate goodness-of-fit (χ^2) values.

Molecular modelling

The molecular docking program Molegro Virtual Docker 2007, was used in conjunction with the E1 ADP bound structure of the Ca^{2+} ATPase SERCA1A (PBD code 1WPE), to predict the potential binding sites for quercetin. This docking programme is based on the algorithm called MolDock which scores potential

sites using differential evolution and cavity prediction, as well as the potential for hydrogen bonding and electrostatic interactions [34]. The highest scoring and most commonly occurring poses for quercetin binding to the Ca^{2+} ATPase were viewed and manually refined using Swiss PBD viewer.

ACKNOWLEDGEMENTS

We thank Ibadan University, Nigeria for a partial a PhD scholarship to O.A.O. Drs Jon Ride & Scott White are also thanked for help with modelling.

REFERENCES

[1] Erlund I, Silaste ML, Alfhan G, Rantala M, & Aro A (2002) Plasma concentrations of flavonoids hesperetin, naringenin and quercetin in human subjects following their habitual diets, and diets high and low in fruit and vegetables, *Eur. J. Clin. Nutr.* **56**, 891-898.

[2] Mense SM, Hei TK, Ganju RK, & Bhat, HK (2008) Phytoestrogens and breast cancer prevention: possible mechanisms of action, *Environ. Health Perspect*. **116**, 426-433.

[3] Syed DN, Khan N, Afaq F, & Mukhtar H (2007) Chemoprevention of prostate cancer through dietary agents: progress and promise, Cancer Epidemiol. Biomarkers. Prev. **16**, 2193-2203

[4] Lechner D, Kallay E, & Cross HS (2005) Phytoestrogens and colorectal cancer prevention, *Vitam. Horm.* **70**, 169-198.

[5] Ramos S (2007) Effects of dietary flavonoids on apoptotic pathways related to cancer chemoprevention, *J. Nutr. Biochem*. **18**, 427-442.

[6] Wang I, Lin-Shiau S, & Lin J (1999) Induction of apoptosis by apegenin and related flavonoids through cytochrome c release and activation of caspase-9 and caspase-3 inleukaemia HL-60 cells, *Eur. J. Cancer*, **35**, 1517-1525.

[7] Khuntawee W, Rungrotmongkol T, & Hannonbuam S (2012) Molecular dynamic behaviour and binding affinity of flavonoid analogues to the cyclin dependent kinase 6 / cyclin D complex. *J. Chem. Inf. Model*. **52,** 76-83

[8] Yuan L, Wang J, Xiao H, Xiao C, & Lui X (2012) isoorientin induces apoptosis through mitochondrial dysfunction and inhibition of the PI3K/Akt signalling pathway in HepG2 cancer cells. *Toxicol. Appl. Pharmacol*. **265**, 83-92.

[9] Lolli G, Cozza G, Mazzorana M, Tibaldi E, Cesaro L, Donella-Deana A, Meggio F, Venerando A, Frachin C, Sarno S, Battistutta R, & Pinna LA (2012) Inhibition of protein kinase CK2 by flavonoids and tyrphostins: A structural insight. *Biochemistry*, **51**, 6097-6107.

[10] Xie F, Lang Q, Zhou M, Zhang H, Zhang Z, Zhang Y, Wan B, Huang Q, & Yu L (2012) The dietary flavonoid luteolin inhibits Aurora B kinase activity and blocks proliferation of cancer cells. *Eur. J. Pharm. Sci.* **46**, 388-396.

[11] Shoshan V & MacLennan DH (1981) Quercetin interaction with the (Ca^{2+}-Mg^{2+})-ATPase of sarcoplasmic reticulum. *J. Biol. Chem.* **256**, 887-892.

[12] Ogunbayo OA, Harris RM, Waring RH, Kirk CJ, & Michelangeli F (2008) Inhibition of the sarcoplasmic / endoplasmic reticulum Ca^{2+}-ATPase by flavonoids: a quantitative structure-activity relationship study. *IUBMB Life.* **60**, 853-858.

[13] Kuhar M, Sen S, & Singh N (2006) Role of mitochondria in quercetin-enhanced chemotherapeutic response in human non-small cell lung carcinoma H-520 cells, *Anticancer Res.* **26**, 1297-1303.

[14] Mouria M, Gukovskaya AS, Jung Y, Buechler P, Hines OJ, Reber HA, & Pandol, SJ (2002) Food-derived polyphenols inhibit pancreatic cancer growth through mitochondrial cytochrome C release and apoptosis, *Int. J. Cancer* **98**, 761-769.

[15] Ogunbayo OA & Michelangeli F (2007) The widely utilized brominated flame retardant tetrabromobisphenol A (TBBPA) is a potent inhibitor of the SERCA Ca^{2+} pump. *Biochem. J*. **408**, 407-415.

[16] Bilmen JG, Wootton LL & Michelangeli, F. (2002) The mechanism of inhibition of the sarco / endoplasmic reticulum Ca^{2+}-ATPase by paxilline. *Arch. Biochem. Biophys.* **406**, 55-64.

[17] Longland CL, Mezna M & Michelangeli F (1999) The mechanism of inhibition of the Ca^{2+}-ATPase by mastoparan. *J. Biol. Chem*. **274**, 14799-14805.

[18] Michelangeli F, Orlowski S, Champeil P, East JM & Lee AG (1990) Mechanism of inhibition of the (Ca^{2+}-Mg^{2+})-ATPase by nonylphenol. *Biochemistry*, **29**, 3091-3101.

[19] Michelangeli F, Colyer J, East JM, & Lee AG (1990) Effect of pH on the activity of the Ca^{2+}-Mg^{2+}-activated ATPase of sarcoplasmic reticulum. *Biochem. J.* **267**, 423-429

[20] Wictome M, Michelangeli F, Lee AG & East JM (1992) The inhibitors thapsigargin and 2,5-di(*tert*-butyl)-1,4-benzohyrdoquinone favour the E2 form of the Ca^{2+}, Mg^{2+}-ATPase. *FEBS Letts*. **304**, 109-113.

[21] Michelangeli F & East JM (2011) A diversity of SERCA Ca^{2+} pump inhibitors. *Biochem. Soc. Trans*. **39**, 789-797.

[22] Froud RJ & Lee AG (1986) Conformational transitions of the Ca^{2+}-Mg^{2+}-activated ATPase and the binding of Ca^{2+} ions. *Biochem. J.* **237**, 197-206.

[23] Yao H, Xu W, Shi X, & Zhang Z (2011) Dietary flavonoids as cancer prevention agents. *J. Environ. Sci. Health C. Environ. Carcinog. Excotoxicol. Rev*. **29**, 1-31.

[24] Logan-Smith MJ, East JM & Lee AG (2002) Evidence for a global inhibitor-induced conformational change on the Ca^{2+} ATPase of sarcoplasmic reticulum from paired inhibitor studies. *Biochemistry*. **41**, 2869-2875

[25] Masuoka N & Kubo I (2004) Characterization of xanthine oxidase inhibition by anacardic acids. *Biochim. Biophys. Acta* **1668**, 245-249

[26] Kessl JJ, Jena N, Koh Y, Taskent-Sezgin H, Slaughter A, Feng L, DeSilva S, Wu L, LeGrice SFJ, Engelman A, Fuchs JR and Kvaratskhelia M (2012) A multimode cooperative mechanism of action of allosteric HIV-1 integrase inhibitors. *J. Biol. Chem.* **287**, 16801-16811

[27] Cody V. & Luft JR (1994) Conformational analysis of flavonoids: crystal and molecular structures of morin hydrate, myricetin (1:2) triphenylphosphine oxide complex. *J. Mol. Struct.* **317**, 89-97

[28] Ma H, Lewis D, Xu C, Inesi G, & Toyoshima C (2005) Functional and structural roles of critical amino acids within the 'N', 'P' and 'A' domains of the Ca^{2+} ATPase (SERCA) headpiece. *Biochemistry,* **44**, 8090-8100.

[29] McIntosh DB, Clausen JD, Woolley DG, MacLennan DH, Vilsen B, & Andersen JP (2003) ATP binding residues of sarcoplasmic reticulum Ca^{2+}-ATPase. *Ann. N.Y. Acad. Sci.* **986**, 101-105.

[30] McIntosh DB, Clausen JD, Woolley DG, MacLennan DH, Vilsen B, & Andersen JP (2004) Roles of conserved P-domain residues and Mg^{2+} in ATP binding in the ground and Ca^{2+}-activated states of sarcoplasmic reticulum Ca^{2+}-ATPase. *J. Biol. Chem.* **279**, 32515-32523.

[31] Autry JM, Rubin JE, Svensson B, Li J, & Thomas DD (2012) Nucleotide activation of the Ca-ATPase. *J. Biol. Chem*. **287**, 39070-39082

[32] Michelangeli F & Munkonge FM (1991) Methods of reconstitution of the purified sarcoplasmic reticulum (Ca^{2+}-Mg^{2+})-ATPase using bile salt detergents to form membranes of defined lipid to protein ratios or sealed vesicles. *Analy. Biochem*. **194**, 231-236.

[33] Gould GW, East JM, Froud RJ, McWhirter JM, Stafanova HI, & Lee AG (1986) A kinetic model for the Ca^{2+}-Mg^{2+}-activated ATPase of sarcoplasmic reticulum. *Biochem. J.* **237**, 217-227.

[34] Thomsen R & Christensen MH (2006) MolDock: a new technique for high-accuracy molecular docking. *J. Med. Chem*. **49**, 3315-3321

Table 1: Inhibitory constants assuming single-site, two-site or cooperative flavonoid binding

Flavonoid	Single site inhibitor binding:	Independent 2-site inhibitor binding:	Cooperative inhibitor binding:
3,6 DHF	Ki = 4.5 ± 0.6μM (χ^2 = 0.92)	Ki^A = 6.2 ± 1.5μM Ki^B = 102 ± 69μM (χ^2 = 0.94)	n= 1.8 ± 0.2 Ki = 5.4 ± 0.3μM (χ^2 = 0.99)
Quercetin	Ki= 9.1 ± 2.7μM (χ^2= 0.86)	Ki^A = 15.9 ± 49μM Ki^B= 21.6 ± 89μM (χ^2= 0.93)	n=2.3 ± 0.3 Ki= 8.7 ± 0.3μM (χ^2= 0.99)
Galangin	Ki= 11.0 ± 2.4μM (χ^2 = 0.85)	Ki^A = 38±147μM Ki^B = 29±87μM (χ^2 = 0.93)	n= 2.2 ± 0.2 Ki= 10.3 ± 0.5μM (χ^2= 0.98)

Table 2: Effects of flavonoids on Ca^{2+} binding parameter monitored by Tryptophan fluorescence changes of the Ca^{2+}-ATPase

	K_d (µM)	k_{on} ($\mu M^{-1}s^{-1}$)	k_{off} (s^{-1})*
Control	0.6±0.1	9.9±0.4	5.9±1.2
Quercetin (20µM)	1.1±0.4	7.4±0.2	8.1±3.2
Galangin (20µM)	0.4±0.1[#]	5.4±0.1	2.1±0.6
3,6-dihydroxyflavone (15µM)	0.3±0.1[##]	7.3±0.2	2.2±0.8

Values are the mean ± SD of 3 determinations for the K_d value and the average of 8 experimental runs for the on rate constant values.

* The Ca^{2+} dissociation rate constant was calculated by multiplying the K_d and the k_{on} values.

[#] $p = 0.07$, [##] $p = 0.03$, compared to control.

Table 3: Changes in FITC-ATPase fluorescence to monitor the E1 to E2 step

(%) change in fluorescence of FITC-Ca^{2+}ATPase

	Control	Quercetin (20µM)	Galangin (20µM)	3,6-dihydroxyflavone (20µM)
Ca^{2+} (400µM)	13.6 ±0.4	1.7±0.3	3.1±0.4	6.2±0.3
(E1/E2 ratio*)	(0.14*)	(8.1)	(4.0)	(1.5)
Vanadate (100µM)	7.0±0.2	9.6±0.2	10.2±0.5	9.3±0.3

* E1/E2 ratio calculated from the Ca^{2+} induced FITC fluorescence changes, assuming a value is 0.14 at pH 6.0 and using the equation described in [22].

LEGENDS

Figure 1: Inhibition of the Ca^{2+}-ATPase activity by flavonoids.

The ATPase activity of the SR Ca^{2+}ATPase activity was measured in a Hepes buffer containing 2.1mM ATP and a free [Ca^{2+}] of 6 µM, at 20 ºC, pH 7.2. The Flavonoids; quercetin (■), 3,6, dihydroxyflavone, 3,6-DHF (▲) and galangin (▼) were added to the assay in DMSO, which never exceeded 1% of the final volume. The figure also includes the structures of the flavonoids used. The solid lines through the data points are the best fits assuming cooperative inhibition, the dotted lines are the best fits to the data assuming a single inhibitor binding site and the dashed lines 2 independent inhibitor binding sites. The inhibition parameters are given in table 1. The data points are the mean ± SD of 3 or more determinations.

Figure 2: Effects of flavonoids on ATPase activity as a function of free [Ca^{2+}]

The ATPase activity was measured in the absence (■) and presence of flavonoids (▲); (A), 3,6 dihydroxyflavone (6 µM); (B), quercetin (9 µM); and (C), galangin (9 µM). The activities were measured in a buffer containing 2.1 mM ATP at pH 7.2 and 20 ºC. The free [Ca^{2+}] was varied from 30 nM to 1.5 mM. The data points represent the mean ± SD of 3 or more determinations.

Figure 3: Effects of flavonoids on the Ca^{2+}-induced changes in tryptophan fluorescence.

The effects of Ca^{2+}-induced tryptophan fluorescence changes in the absence (●) and presence of 20 µM flavonoids; quercetin (■), galangin (▼) and 3,6 dihydroxyflavone (▲) were measured at pH 7.0 and 20 ºC. The changes were measured over a range of free Ca^{2+} concentrations (10 nM to 0.1 mM). The calculated K_d values are presented in Table 1. The data points represent the mean ± SD of 3 determinations.

Figure 4: Effects of flavonoids on Ca^{2+} ATPase activity as a function of [ATP].

The ATPase activity was measured in a Hepes buffer, pH 7.2 at 20 ºC, containing 6 µM free [Ca^{2+}] and a range of ATP concentrations (0.18 µM to 2.3 mM). The activities were measured in the either the absence of flavonoids (●), or in the presence of quercetin (■); galangin (▼) or 3,6 dihydroxyflavone (▲). The data points are the mean ± SD of 3 or more determinations.

Figure 5: Effects of flavonoids on ATP binding.

ATP binding was measured at pH 7.0 and 3 ºC. 0.5 mg/ml (5 µM) Ca^{2+} ATPase was incubated in the buffer containing [^{32}P]ATP (125 Ci/mol) and in the absence or presence of 50 µM of galangin, quercetin or 3,6 dihydroxyflavone (3,6DHF). The values represent the the mean ± SD of 8 determinations.

Figure 6: Effects of flavonoids on the rates of phosphorylation and dephosphorylation.

(A) shows the levels of phospho-enzyme intermediate (E-P) formed when the Ca^{2+} ATPase was incubated in a buffer at pH 7.0 , 3 ºC and [^{32}P]ATP (20 Ci/mol) added prior to stopping the reaction after 10 s and 30 s. The experiments were performed in the absence or the presence of 30 µM, quercetin, galangin and 3,6 dihydroxyflavone (3,6DHF). The values present the mean ± SD of 3 determinations.

(B) Shows the phospho-enzyme intermediate decay measured at pH 7.0, 3 ºC. The Ca^{2+} ATPase (0.15 mg/ml) was allowed to reach steady state levels of phosphorylation by initiating the reaction with [^{32}P]ATP (20 Ci/mol), after which excess non-radioactive ATP (0.5 mM) was added and the E-P levels monitored by stopping the reaction at various time points (ie 0 to 20 s) following its addition. The experiments were performed in the absence (●) of flavonoids or in the presence of 30 µM of; quercetin

(■), galangin (▼) or 3,6 dihydroxyflavone (▲). The data points represent the mean ± SD of 3 determinations.

7: The effects of flavonoids on the ratio of ADP-sensitive to ADP-insensitive forms of the Ca^{2+} ATPase.

The experiments were performed at pH 7.2 and 3 ºC. Ca^{2+}ATPase (0.1 mg/ml) was phosphorylated by the addition of 20 μM [^{32}P]ATP (20 Ci/mol) for up to 40 s, following which 1.5 mM ADP was added. Samples were taken at 5 s intervals post ADP addition (arrow) and the E-P levels measured. The experiments were performed in the absence of flavonoids (○) or in the presence of 30 μM of; quercetin (□), galangin (▽) or 3,6 dihydroxyflavone (△). The data points represent the mean ± SD of 3 determinations.

8: Modelling of the flavonoid binding sites on the Ca^{2+} ATPase.

Molegro Virtual Docker 2007 programme was used to predict the quercetin binding sites within the E1.ADP bound form of the SERCA1 Ca^{2+} ATPase structure (PBD 1WPE).

(A) Shows that quercetin can adopt a kinked conformation that can be substantially superimposed onto the structure of ADP as adopted when bound to the Ca^{2+} ATPase. (B) Shows two potential binding sites for quercetin. Site 1 is within the nucleotide binding domain (N-domain) and site 2 at the interface between the N-domain and a actuator domain (A-domain). (C) Shows the potential interactions of quercetin with key amino acid residues within site 1 (H-bonds highlighted by dashed lines). (D) shows the location of ADP within sites 1. (E) shows the predicted binding site 2 and also highlights key amino acids that can for potentially form H-bond with quercetin.

FIG1

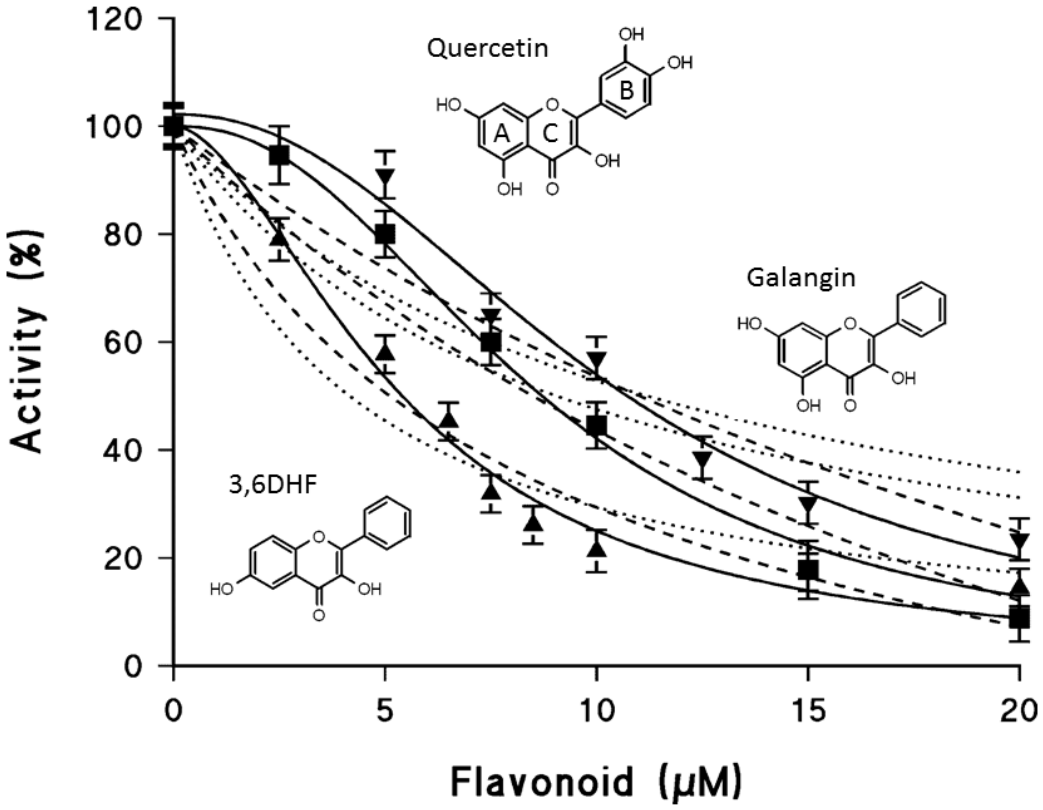
Quercetin
Galangin
3,6DHF
Activity (%)
Flavonoid (μM)
0
20
40
60
80
100
120
0
5
10
15
20

FIG2

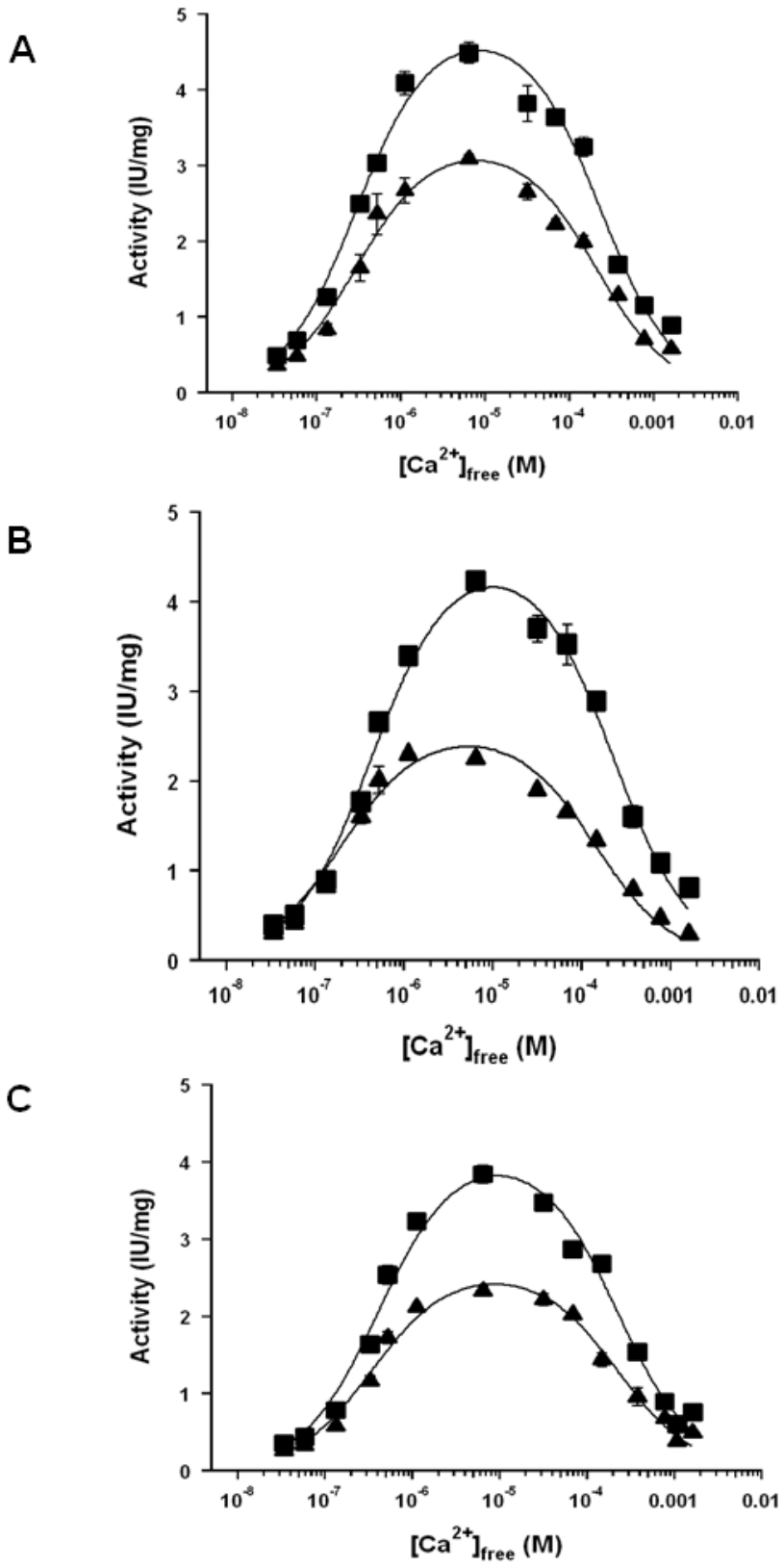
A
B
C
Activity (IU/mg)
[Ca2+]free (M)
0
1
2
3
4
5
10-8
10-7
10-6
10-5
10-4
0.001
0.01

FIG3

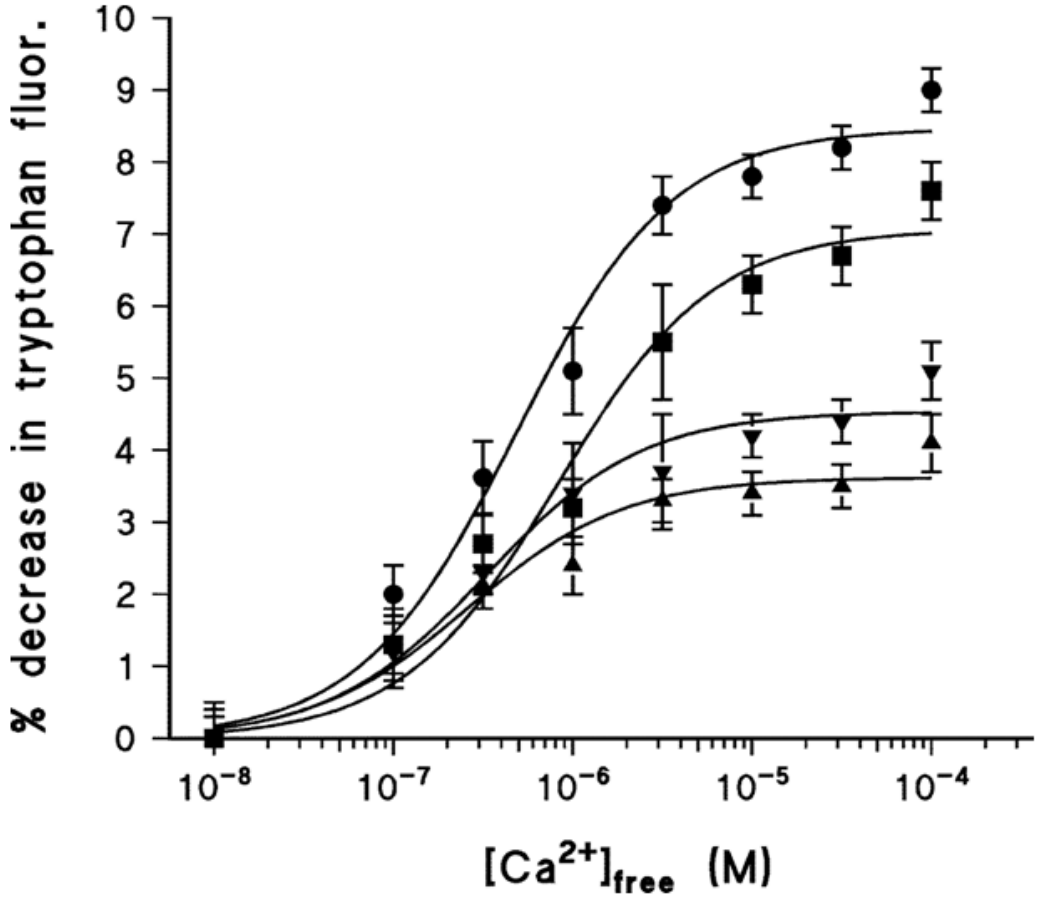
% decrease in tryptophan fluor.
10
9
8
7
6
5
4
3
2
1
0
10^{-8}
10^{-7}
10^{-6}
10^{-5}
10^{-4}
$[Ca^{2+}]_{free}$ (M)

FIG4

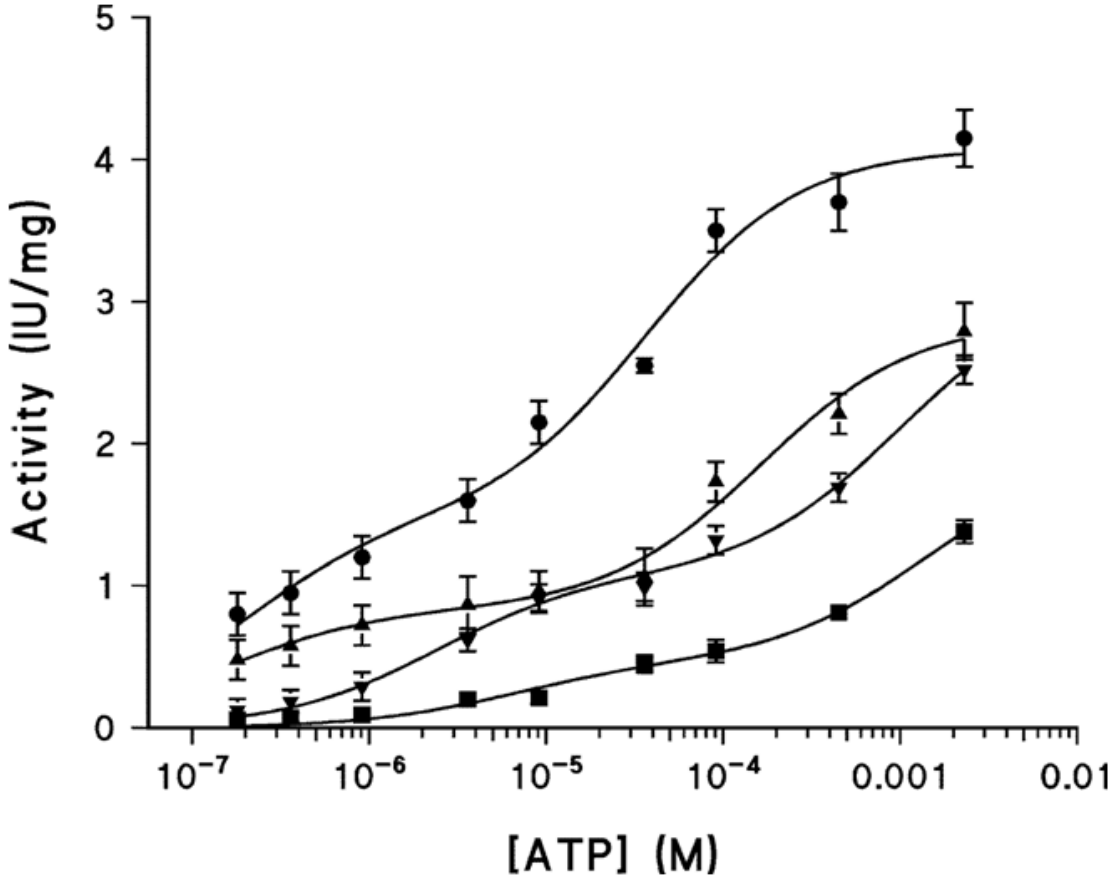

FIG 5

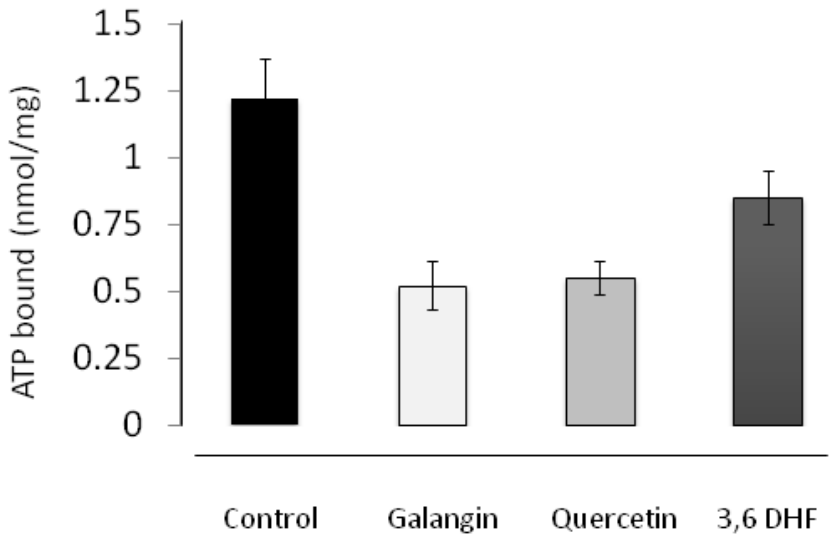
ATP bound (nmol/mg)
1.5
1.25
1
0.75
0.5
0.25
0
Control
Galangin
Quercetin
3,6 DHF

FIG6

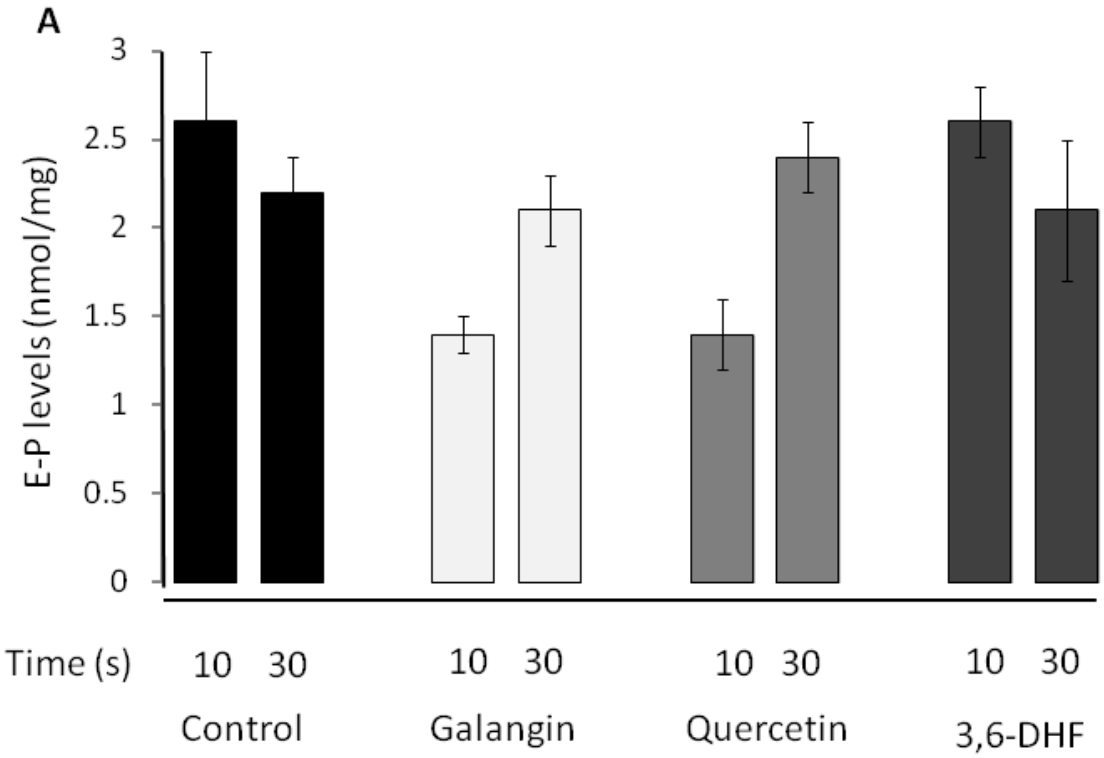
A
E-P levels (nmol/mg)
3
2.5
2
1.5
1
0.5
0
Time (s)
10 30
10 30
10 30
10 30
Control
Galangin
Quercetin
3,6-DHF

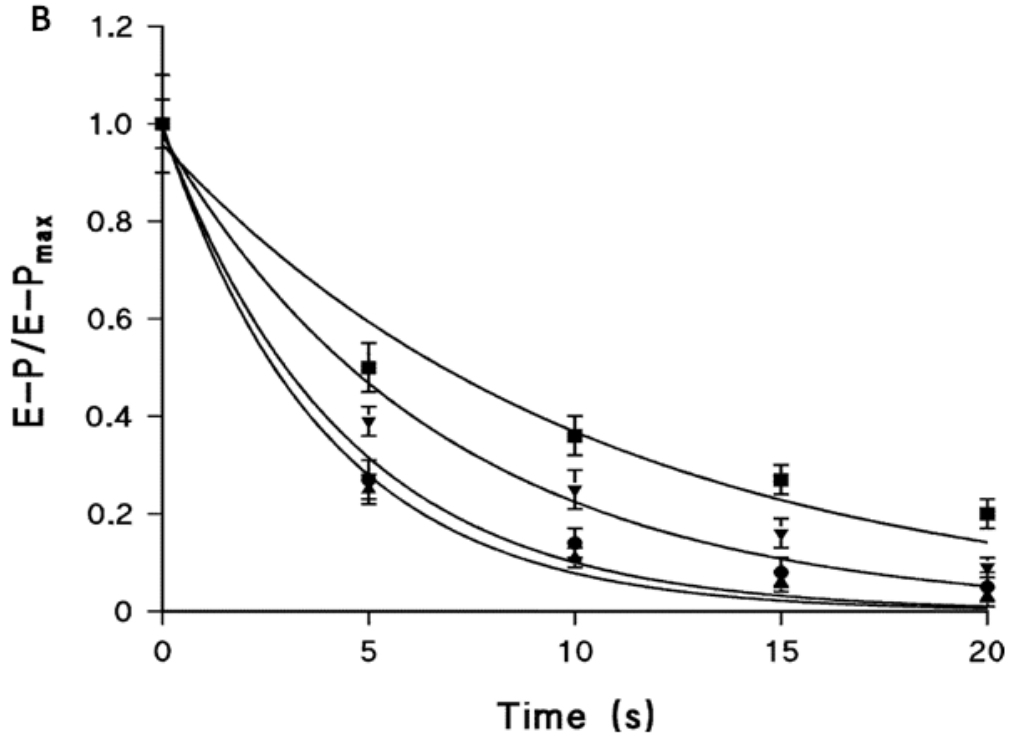
B
E–P/E–P max
1.2
1.0
0.8
0.6
0.4
0.2
0
0
5
10
15
20
Time (s)

FIG7

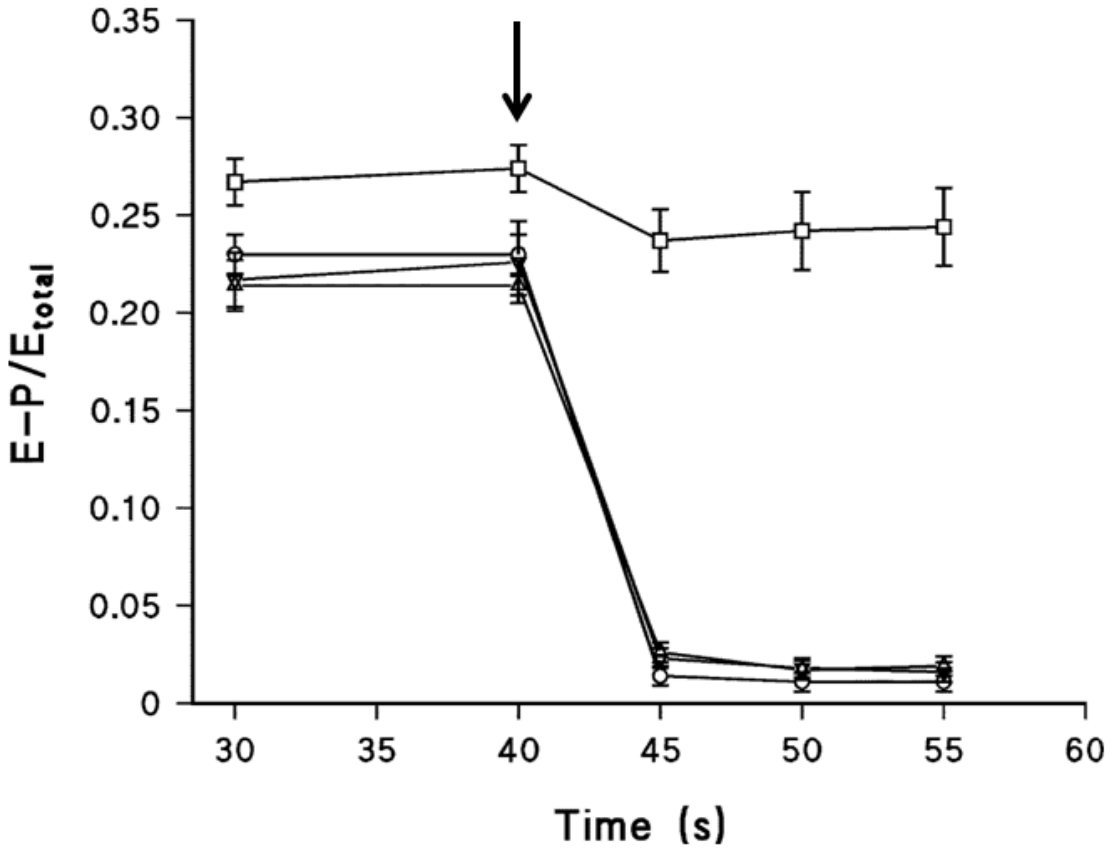

FIG 8

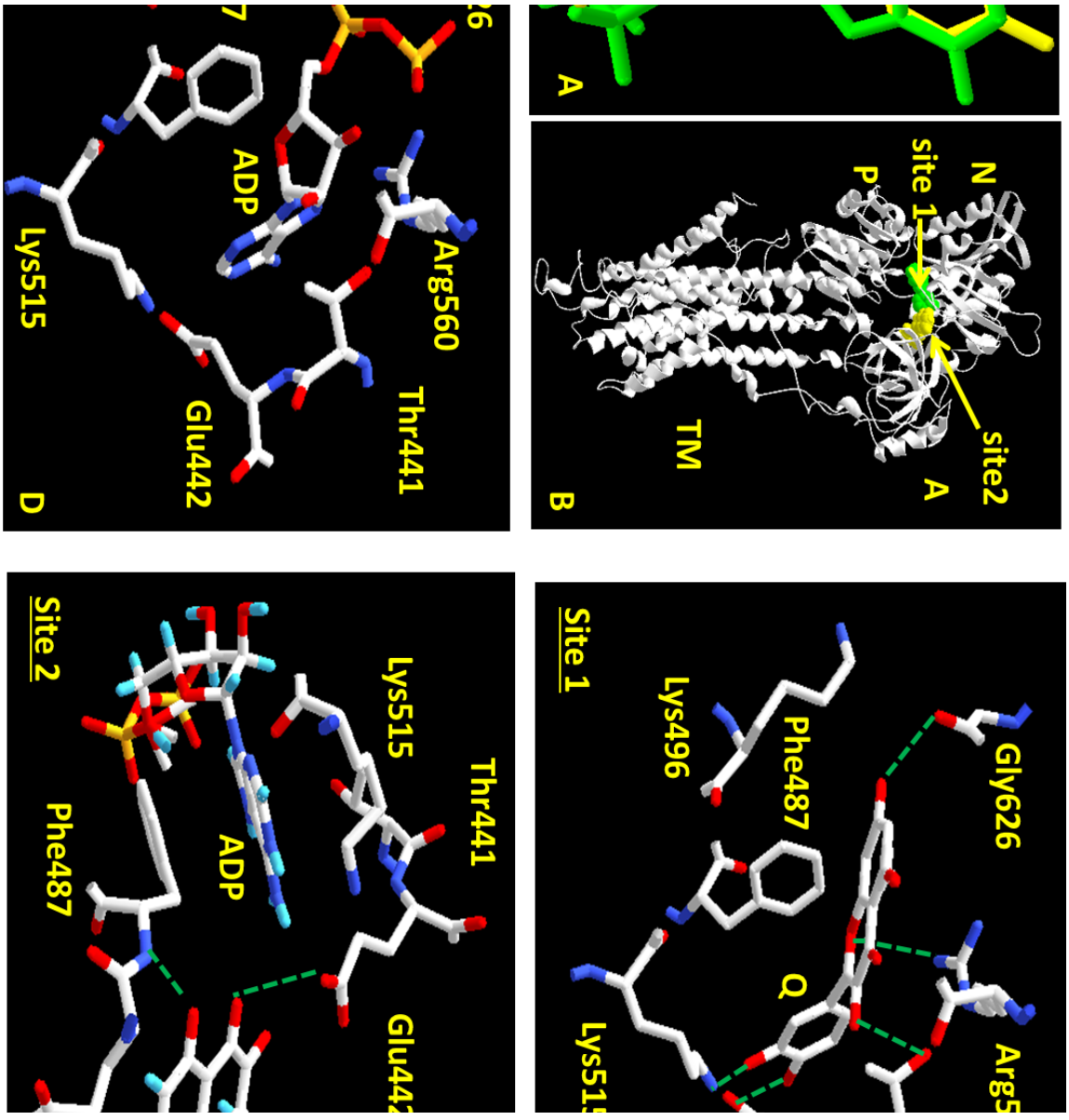
A
N
site 1
P
site2
A
TM
B
Arg560
ADP
Thr441
Lys515
Glu442
D
Gly626
Site 1
Lys496
Phe487
Q
Site 2
Lys515
Thr441
ADP
Phe487